Send Orders for Reprints to reprints@benthamscience.ae

The Open Automation and Control Systems Journal, 2015, *7*, 1993-2000

Computer Image Feature Extraction Algorithm for Robot Visual Equipment

Wang Li*

College of Computer and Information Engineering, Tianjin Chengjian University, Tianjin, China

Abstract: To improve the poor condition of the robot image feature extraction with change in the environment, this thesis made improvement in the Local Binary Patterns (LBP), and proposed the SIFT-MLBP image feature extraction, coding by partition grid based on the correlation between the neighboring image center pixel points. After obtaining the key image characteristics by using the SIFT algorithm, a gridding structure was built centered on the pixel point in each region, calculating the partial difference between the pixel points, and assigning weight to each pixel encoding with different contrasts. In this study, the model-based feature vector combining the Gabor algorithm was extracted to build the SIFT-GMLBP feature vector, which reduced feature dimensions by mapping of the original complement with each other. The test showed that the SIFT-GMLBP algorithm possesses a fairly good feature matching effect, with the correct matching rate over 95%, and reduced running time of 0.05S. The robustness of this method in dealing with the external environment is quite remarkable, as it is able to improve the speed and precision of the mobile robots' image identification in the complex environment.

Keywords: Feature extraction, Grid, Local Binary Patterns (LBP), Visual pattern.

1. INTRODUCTION

The visual pattern feature extraction is a key technology for the robot to perceive and identify the external environment. The robot can realize the navigation and target-action through the environmental message operation. The current, fast and precise image information acquisition is of great significance to the mobile robots. However, the current visual pattern feature extraction algorithm is not that good with complex background, great contrast and loud noise, therefore it was required to improve the current algorithm, to enhance the environment identification capacity of mobile robots. The image matching SIFT algorithm based on local features is widely applied [1, 2] in the robot visual pattern feature extraction, but the sub-dimension of SIFT feature description is quite high, which increases the computational complexity and time complexity. Literature [3] highlights the optimization of SIFT by using the Difference of Gaussians (DOG) and area detection method, thus increasing the arithmetic speed. According to the literature [4, 5], SIFT is easily influenced by image noises and brightness variations, therefore, the study proposed the improvement methods. However, when there is a great contrast between the SIFT algorithm and the original image, the matching effect is not that good. Many studies have improved SIFT in a constant way, and combined other pattern feature extraction algorithms. The LBP and its variations have already been successfully applied for various texture recognition, face recognition, visual speech recognition, *etc*. [6-11]. The [12] combination of SIFT and the rotation invariant LBP has also been reported, which increased the robustness of the illumination invariance, with greater vector dimension of the rotation invariant LBP, leading to increase in the calculated amount. Literature [13] and [14] reported improved traditional LBP using DRLBP and LMEP, which increased the distinguishing ability of the complex background. The study [15-17] combined the Gabor and the LBP, possessing great texture detection feature, with the drawback of computing being quite complex.

This thesis studied the SIFT feature description and the LBP combined feature extraction method, using the mesh generation center pixel point and the different pixel weight, to improve the LBP. This thesis built a feature vector by combining Gabor wavelet algorithm, and reduced the vector dimension through the original code complement mapping. The result of the mobile robot visual image feature matching extraction experiment showed that both the matching accuracy and the operating time were improved, which was suitable for the mobile robot visual image feature extraction.

2. SIFT FEATURE DESCRIPTION OPERATOR

The SIFT algorithm based on the scale space theory is a local feature extraction algorithm. It is a process of extracting key SIFT points from the images. It can extract the local features from three basic aspects, the dimension, direction and size in the image, possessing great peculiarities, quantities and particularities. The basic model of the SIFT algorithm is shown in Fig. (**1**).

This algorithm mainly includes the following 4 steps: Scale space extreme point detection, location positioning of key points, the principal direction of key points positioning, and feature descriptor generation.

*Address correspondence to this author at the College of Computer and Information Engineering, Tianjin Chengjian University, Tianjin, 300384, China; Tel: 13821773575; Fax: 02588574154;
E-mail: kkkwangli@163.com

1874-4443/15

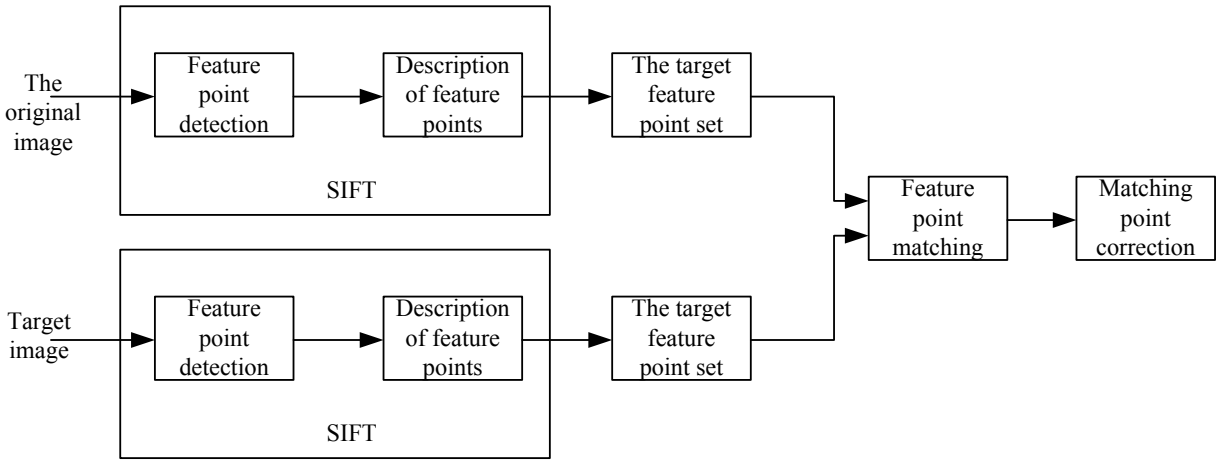

Fig. (1). The basic model of SIFT algorithm.

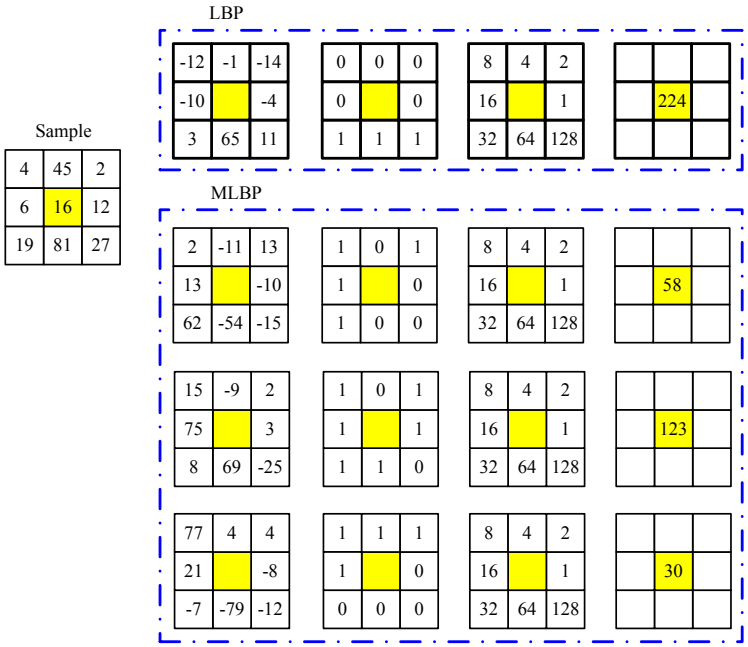

Fig. (2). The binary pattern of LBP and MLBP in the 3×3 neighborhood.

First, a Gaussian scale space image is created, that is the Gaussian pyramid, which detects the local minimums possessing directional information in the images under different scale spaces. Subtracting the neighborhood spatial functions of Gaussian pyramid, the Difference of Gaussian (DOG) pyramid is obtained . Since the value of DOG is sensitive to the noises and the margin, to obtain the final stable image feature points, positions of the local minimums detected by the DOG scale space are further examined in terms of the candidate key points. To assign the direction parameter to each feature, a key point is assigned based on neighborhood pixel and distribution features of the gradient direction, to esure the rotation invariance of operators. After the above steps, the required stable image feature points can be detected and the information related to each feature point is obtained, to set a feature description operator for each key point, for determining the feature vector. In addition, each dimension of the feature vectors should be limited to a certain range of threshold. If the value of one dimension surpasses this range, the result should be equal to this threshold, and the vector should be normalized once again. Therefore, the final SIFT feature descriptor can be obtained.

3. FEATURE DETECTION OF MLBP ALGORITHM

3.1. LBP Algorithm

In terms of the LBP algorithm, the gray value of the image local center pixel is the threshold value, and the binary coding can be acquired by comparison with its neighborhood pixel gray value to describe the local texture feature. The 3×3 neighborhood binary coding is shown in Fig. (**2**).

To expand the basic LBP 3×3 neighborhood to a wide neighborhood, choosing a circular neighborhood with the radius being R, and selecting P evenly as spaced points on the circle, binarization can be done after a comparison between the gray value of the P points and that of the central point. The coordinate of the P points can be determined by the flowing formula (1).

$$(x_k, y_k) = (x_c + R\cos(2\pi k/P), y_c - R\sin(2\pi k/P))$$
$$(k = 1,2,\text{L}\ ,P) \tag{1}$$

Where the (x_k, y_k) stands for the coordinate of the K th, and x_c and y_c are the abscissa and ordinate, respectively, of the central pixel.

If $x_k = i+u, y_k = j+v$, where i and j are all non-negative integers, u and v are the floating points in the section [0,1], the pixel value g(i+u,j+v) of this point can be determined by four corresponding pixel values (i,j)、(i+1,j)、(i+1,j)、(i+1,j+1) in the image, as shown in formula (2):

$$\begin{aligned} g(i+u, j+v) &= (1-u)(1-v)g(i,j) \\ &+ (1-u)vg(i,j+1) \\ &+ u(1-v)g(i+1,j) + uvg(i+1,j+1) \end{aligned} \tag{2}$$

Where g(i,j) stands for the pixel value of the point (i,j) in the original image.

If the gray value of the central pixel point is g_c, and the gray value of the P sampling points is g_1, g_2, …, g_p, respectively, the computational formula for the characteristic value of the LBP surrounding the central pixel point is shown in formula (3):

$$LBP_{P,R} = \sum_{i=1}^{P} 2^{i-1} S(g_i - g_c) \tag{3}$$

Where, $S(x) = \begin{cases} 1, x \geq 0 \\ 0, x < 0 \end{cases}$.

In this thesis, in terms of the characteristics of LBP ($LBP_{8,1.0}$), P=8,R=1.0, the operators of $LBP_{P,R}$ can produce 2^P different binary modes.

3.2. MLBP Operator Construction

As the combination of SIFT and LBP can greatly increase the dimension of feature vectors, the searching of feature vectors will be more complex, and will be more sensitive to the noise and small fluctuations of pixel value, leading to the poor detection effect of the image with greater contrast. To solve this problem, the discriminating degree of local similarity characteristics should be enhanced. In addition, this thesis proposed the Mesh LBP (MLBP) on the basis of LBP algorithm, meshing and encoding according to the relationship of the central pixel points neighbourhood of the given image. Also, the extraction of complex image characteristics was realized through the combination of Gabor transforming, reducing the dimension of the feature vectors. The computational formula of the central pixel point surrounding 3×3 neighborhood MLBP eigenvalue is shown in formula (4):

$$MLBP_{P,R}^{j} = \sum_{i=1}^{P} 2^{i-1} S(g_\alpha - g_i) \tag{4}$$

Where, $\alpha = 1 + \text{mod}((i+P+j-1), P)$, $j = 1,2,...,P/2$, and mod （） is the remainder of the central pixel point ratio of the horizontal ordinate.

With the formula (4), it can be observed that there are P/2 neighborhoods of P sampling points in MLBP. The binary encoding of the first three models of MLBP （j=1,2,3） studied in this thesis is shown in Fig. (**2**). The neighborhood model of LBP and MLBP in the 3×3 neighborhood with given (P, R) is shown in Fig. (**3**).

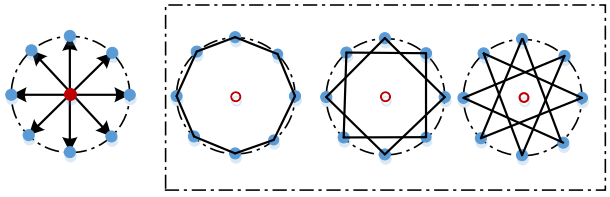

Fig. (3). The neighborhood model of LBP and MLBP when P=8, R=1.0.

Generally, the distinctions between different targets mainly rely on the distinction of surface texture and shape. In particular, the expression is more obvious with the marginal area.

$$\omega_{x,y} = \sqrt{I_x^2 + I_y^2} \tag{5}$$

Where: I_x, and I_y are the first derivatives in x and y directions of the pixel.

The greater the contrast of the pixels, the larger the weight of the pixels' MLBP encoding . The i dimension eigenvalue of M*N pixel block MLBP feature is shown as the formula (6).

$$MLBP_i = \sum_{x=0}^{M-1} \sum_{y=0}^{N-1} \omega_{x,y} \delta(MLBP_{x,y}, i) \tag{6}$$

Where $\delta(m,n) = \begin{cases} 1, m = n \\ 0, m \neq n \end{cases}$

This thesis extracted the model-based feature vector combining the Gabor transformation. The Gabor transformation is the Windowed Fourier Transform, in which the Gabor function is able to extract related characteristics in the frequency domain with different scales and different directions. In addition, the Gabor function is similar to the

human eyes' biological action, therefore, it is often used for texture recognition, to achieve good result. The Gaussian envelope expressed by frequency ω, and the standard deviations σ_x and σ_y are shown as formula (7):

$$\psi(x,y)=\frac{1}{2\pi\sigma_x\sigma_y}e^{[-(1/2)(x^2/\sigma_x^2+y^2/\sigma_y^2)+2\pi j\omega x]} \tag{7}$$

With the scaling and rotation of the above formula, the Gabor wavelet expression can be acquired as shown in formula (8).

$$\psi_{mn}(x,y)=a^{-m}\psi(x',y') \tag{8}$$

Where: $m\in\{0,...,S-1\}, n\in\{0,...,K-1\}$ which show the scale and direction, respectively, with K and S being the expected value of scale and direction, respectively.

$$a=(U_h/U_l)^{-1/s-1}, \omega_{m,n}=U_h \tag{9}$$

$$\sigma_{x,m,n}=\frac{(a+1)\sqrt{2\ln 2}}{2\pi a^m(a-1)U_l} \tag{10}$$

$$\sigma_{y,m,n}=\frac{1}{2\pi\tan(\frac{\pi}{2k})\sqrt{\frac{U_h^2}{2\ln 2}-(\frac{1}{2\pi\sigma_{x,m,n}})^2}} \tag{11}$$

Where, U_h and U_l are the upper and lower cutoff frequencies of the design band, respectively, with U_h=0.05, and U_l=0.49.

With the convolution of Gabor window and image, the response expression for the Gabor filter can be acquired, as shown in the flowing equation.

$$G_{mn}(x,y)=\sum_s\sum_t(x-s,y-t)\psi^*_{mn}(s,t). \tag{12}$$

This thesis utilized Gabor wavelet transform (WT) for the calculation of MLBP characteristic mapping (GMLBP). For the central point with given coordinate, such as P=8, R=1.0. The characteristic mapping of GMLBP when j=1 can be shown as (13).

$$GMLBP^1_{8,1.0}=\begin{cases}S(G_{45^\circ}(x-R,y+R)-G_{0^\circ}(x,y+R))\\ S(G_{90^\circ}(x-R,y)-G_{45^\circ}(x-R,y+R))\\ S(G_{135^\circ}(x-R,y-R)-G_{90^\circ}(x-R,y))\\ S(G_{0^\circ}(x,y-R)-G_{135^\circ}(x-R,y-R))\\ S(G_{45^\circ}(x+R,y-R)-G_{0^\circ}(x,y-R))\\ S(G_{90^\circ}(x+R,y)-G_{45^\circ}(x+R,y-R))\\ S(G_{135^\circ}(x+R,y+R)-G_{90^\circ}(x+R,y))\\ S(G_{0^\circ}(x,y+R)-G_{135^\circ}(x+R,y+R))\end{cases} \tag{13}$$

3.3. SIFT-GMLBP Feature Extraction

When the image background is complex, or polluted by noises, the searching effect of the SIFT algorithm is not that good. In contrast, the GMLBP possesses the illumination invariants and features of meshing feature extraction , therefore, it can filtrate the noise pollution of the image, and increase the degree of similarity of local similarity characteristics, thus making up for the deficiency of SIFT algorithm in aspects like image pollution and brightness invariance. The robustness of image texture recognition in different scales and directions can also be enhanced at the same time.

The process of the formation of SIFT-GMLBP feature description is as follows:

Step 1: The feature key points are detected based on the detection method of the SIFT key points. $p_i(h,v,\sigma,\theta)$ is detected as the key points, where (h,v) is the position coordinate of the key point on the original image, with σ and θ being the scale and direction of the key point.

Step 2: With the key point p_i as the center, the feature vector $SIFT_i$ is set with 128 dimensions in an area of 16×16 size.

Step 3: With the key point p_i as the center, the meshing structure is centered every pixel point in the neighborhood by selecting an area of 9×9 size in the surrounding followed by the calculation of local differences of the neighborhood pixels.

Step 4: The MLBP feature is built as $MLBP_{8,1.0}$ with P=8, and R=1.0, and MLBP's binary pattern is calculated. The feature vector extraction is carried out by using the Gabor transformation, to obtain the 81 dimensions feature $GMLBP_i$.

$$GMLBP_i=[GMLBP^1_{8,1.0}\ GMLBP^2_{8,1.0}\cdots GMLBP^{81}_{8,1.0}] \tag{14}$$

Step 5: A new 128 dimensions feature vector $(SIFT-MLBP)_i=[SIFT_i\ MLBP_i]$ is formed by combining $SIFT_i$ and $GMLBP_i$.

Step 6: Mutual mapping is performed between the GMLBP original code and the complement, with the minimum value, is shown as formula (15):

$$GMLBP_{x,y}=\min\{GMLBP_{x,y},2^B-1-GMLBP_{x,y}\} \tag{15}$$

Due to equal division of the original code with mapping, if B=8, the amount of GMLBP features will be reduced from 128 dimensions to 59 dimensions when using the original code of the united model.

Step 7: To give each code a weight $\omega_{XY,}$ the produced features will include the marginal and textural information of the single representation after adding the weight to the GMLBP coding. Finally, 59 dimensions of vector $(SIFT-GMLBP)_i$ are obtained , that form the feature description of the key point p_i of the surrounding area.

Fig. (4). The ability storm robot (AS-R).

Fig. (5). The extraction of image key points.

4. PERFORMANCE TEST ANALYSIS FOR THE FEATURE VECTORS

The test utilized the Ability Storm Robot (AS-R) to perform experimental testing by taking pictures in the real environment. The robot is shown in Fig. (**4**). Key points extraction of the image with Yuntai camera is shown in Fig. (**5**). Altogether, there were 64 key points extracted after removing the marginal, border-close and low contrast points.

As shown in Fig. (**6a-d**), to conduct the feature matching of the obtained images with scale variations, rotations variations, view changes and illumination variations, the SIFT-GMLBP algorithm was utilized.

In Fig. (**6a**), the correcting points and the total points were 62/64 when zooming was 0.25 times, with the correct matching rate being 96.88%. In Fig. (**6b**), the correct matching rate is shown to be 63/64=98.44% after rotating 20 degrees. In Fig. (**6c**), the correct matching rate is 61/64=95.31 % after view variation. In Fig. (**6d**), the correct matching rate is 63/64=98.44% after dimming of the light. The feature extraction by the SIFT-GMLBP algorithm can maintain the invariance of image scale, rotation and view translation, and possess great robustness for the illumination variations, reinforcing the distinction of the image intensity contrast.

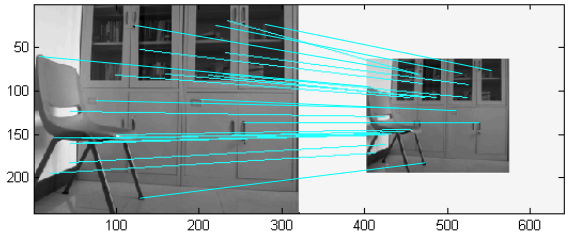

(**a**) The scale variations matching

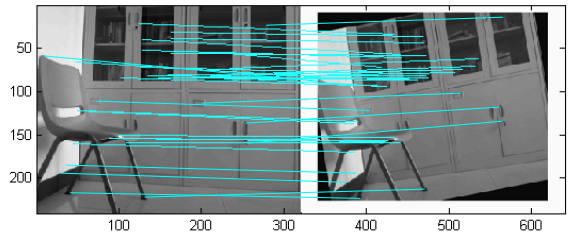

(**b**) The rotation variations matching

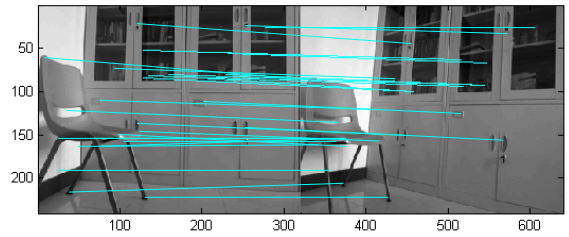

(**c**) The view variations matching

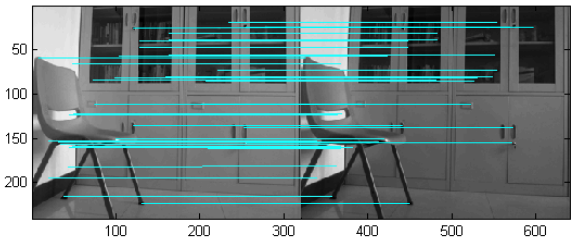

(**d**) The illumination variations matching

Fig. (6). The feature matching result of SIFT-GMLBP algorithm.

Fig. (**7**) shows the PVR curve based on the recall ratio and the precision ratio of the four methods' image matching. The larger the area enclosed by the curve and the coordinate axis, the better is the performance. Therefore, image matching performance of this algorithm is better than that of other algorithms.

In terms of time performance, with the application of the mutual mapping of the original code and the complement, as well as the minimum value, the vector dimension is reduced, and the general operating time greatly reduced compared with the SIFT algorithm. Table **1** lists the comparison between different algorithms.

Table 1. The Operating Time of Different Algorithms.

Algorithms	Operating Time
SIFT	0.9279s
SIFT-LBP	0.9640s
SIFT-GMLBP	0.8764s

CONCLUSION

To improve the robots' recognition speed and precision in complex environment, this thesis replaced the LBP

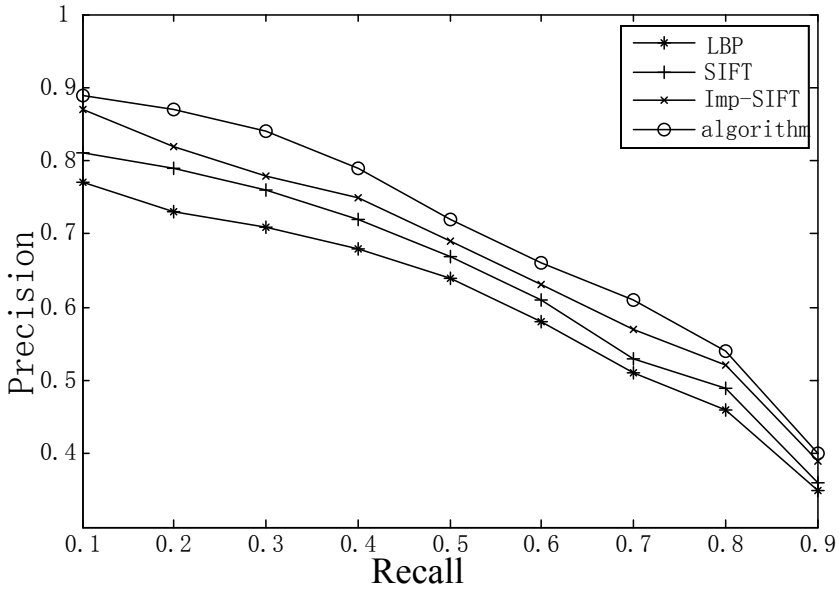

Fig. (7). The four methods' recall ratio and precision ratio curve.

neighborhood partition with the meshing, on the basis of SIFT-LBP algorithm, and improved the texture feature extraction method as well as the vector dimensions. Both the matching speed and precision improved to a certain extent based on the excellent scale, rotation, view and illumination of the SIFT-GMLBP image feature extraction in complex environment, with the experiment of the robots' actual image gathering. There is a certain application value of the mobile robots for target identification and route planning.

CONFLICT OF INTEREST

The author confirms that this article content has no conflicts of interest.

ACKNOWLEDGEMENTS

This paper was supported by Tianjin Municipal Natural Science Foundation, No. 11JCYBJC00900.

REFERENCES

[1] M. Zhang, Z. Lv, X. Zhang, G. Chen, and K. Zhang, "Research and Application of the 3D Virtual Community Based on WEBVR and RIA," *Computer and Information Science,* vol. 2, no. 1, pp. 84, 2009.

[2] T. Su, Z. Lv, S. Gao, X. Li, and H. Lv, "3D seabed: 3D modeling and visualization platform for the seabed," In*: Multimedia and Expo Workshops (ICMEW)*, International Conference on, pp. 1-6, 2014.

[3] X. Li, Z. Lv, B. Zhang, W. Wang, S. Feng, and J. Hu, "WebVRGIS Based City Bigdata 3D Visualization and Analysis," In: *Pacific Visualization Symposium (PacificVis)*, 2015.

[4] S. Li, Y. Geng, J. He, K. Pahlavan, "Analysis of Three-dimensional Maximum Likelihood Algorithm for Capsule Endoscopy Localization," 5th International Conference on *Biomedical Engineering and Informatics* (BMEI), Chongqing, China, pp. 721-725, 2012.

[5] Y. Geng, J. He, H. Deng and K. Pahlavan, "Modeling the Effect of Human Body on TOA Ranging for Indoor Human Tracking with Wrist Mounted Sensor," 16th International Symposium on *Wireless Personal Multimedia Communications* (WPMC), Atlantic City, NJ, 2013.

[6] G. N. Brock, J. R. Shaffer, R. E. Blakesley, M. J. Lotz, and G. C. Tseng, "Which missing value imputation method to use in expression profiles: a comparative study and two selection schemes," *BMC Bioinformatics*, vol. 9, pp.12, 2008.

[7] Y. Saeys, I. Lnza, and P. Larrañaga, "A review of feature selection technique in bioinformatics," *Bioinformatics*, vol. 23, no.19, pp.2507-2517, 2007.

[8] T. R. Golub, D. K. Slonim, P. Tamayo, C. Huard, M. Gaasenbeek, J.P. Mesirov, H. Coller, M. L. Loh, J.R. Downing, M.A. Caligiuri, C.D. Bloomfield, and E.S. Lander, "Molecular classification of cancer: class discovery and class prediction by gene expression monitoring," *Science*, vol. 286, no. 5439, pp.531-537, 1999.

[9] L. Li, C. R. Weinberg, T. A. Darden, and L. G. Pedersen, "Gene selection for sample classification based on gene expression data: study of sensitivity to choice of parameters of the GA/KNN method," *Bioinformatics*, vol. 17, no.12, pp. 1131-1142, 2001.

[10] X. W. Chen, "Margin-based wrapper methods for gene identification using microarray," *Neurocomputing*, vol. 69, no.16-18, pp. 2236-2243, 2006.

[11] D. U. Ramón, and A. A. Sara, "Gene selection and classification of microarray data using random forest," *BMC Bioinformatics*, vol. 7, pp. 3, 2006.

[12] S. G. Ma, X. Song, and J. Huang, "Supervised group Lasso with applications to microarray data analysis," *BMC Bioinformatics*, vol. 8, no.60, 2007.

[13] R. Tibshirani, "Regression shrinkage and selection *via* the Lasso," *Journal of the Royal Statistical Society Series B-Methodological*, vol. 58, no. 1, pp.267-288, 1996.

[14] B. Efron, T. Hastie, I. Johnstone, "Least Angle Regression," *Journal of the Institute of Mathematical Statistics*, vol. 32, no. 2, pp. 407-499, 2004.

[15] D. Singh, P. G. Febbo, K. Ross, D. G. Jackson, J. Manola, C. Ladd, P. Tamayo, A.A. Renshaw, A. V. D'Amico, J. P. Richie, E. S. Lander, M. Loda, P.W. Kantoff, T.R. Golub, and W. R. Sellers, "Gene expression correlates of clinical prostate cancer behavior," *Cancer Cell*, vol. 1, no. 2, pp. 203-209, 2002.

[16] Y. D. Zhao, and R. Simon, "BRB-ArrayTools Data Archive for Human Cancer Gene Expression: A Unique and Efficient Data Sharing Resource," *Cancer Informatics*, vol. 6, pp. 9-15, 2008.

[17] M. P. S. Brown, W. N. Grundy, D. Lin, N. Cristianini, C.W. Sugnet, T. S. Furey, M. J. Ares, and D. Haussler, "Knowledge-based analysis of microarray gene expression data by using support vector machines," In: *Proceedings of the National Academy of Sciences of the United States of America*, vol. 97, no. 1, pp.262-267, 2000.

Received: June 16, 2015 Revised: August 10, 2015 Accepted: September 19, 2015